The Astrophysical Journal Letters, 764:L10 (5pp), 2013 February 10 doi:10.1088/2041-8205/764/1/L10

SMALL-SCALE STRUCTURE OF THE INTERSTELLAR MEDIUM TOWARD ρ Oph STARS: DIFFUSE BAND OBSERVATIONS

M. A. Cordiner[1,3], S. J. Fossey[2], A. M. Smith[1,4], and P. J. Sarre[1]
[1] School of Chemistry, The University of Nottingham, University Park, Nottingham NG7 2RD, UK; martin.cordiner@nasa.gov
[2] Department of Physics and Astronomy, University College London, Gower Street, London WC1E 6BT, UK
Received 2012 November 17; accepted 2013 January 6; published 2013 January 28

ABSTRACT

We present an investigation of small-scale structure in the distribution of large molecules/dust in the interstellar medium through observations of diffuse interstellar bands (DIBs). High signal-to-noise optical spectra were recorded toward the stars ρ Oph A, B, C, and DE using the University College London Echelle Spectrograph on the Anglo-Australian Telescope. The strengths of some of the DIBs are found to differ by about 5%–9% between the close binary stars ρ Oph A and B, which are separated by a projected distance on the sky of only *c.* 344 AU. This is the first star system in which such small-scale DIB strength variations have been reported. The observed variations are attributed to differences between a combination of carrier abundance and the physical conditions present along each sightline. The sightline toward ρ Oph C contains relatively dense, molecule-rich material and has the strongest $\lambda\lambda$5850 and 4726 DIBs. The gas toward DE is more diffuse and is found to exhibit weak "C_2" (blue) DIBs and strong yellow/red DIBs. The differences in diffuse band strengths between lines of sight are, in some cases, significantly greater in magnitude than the corresponding variations among atomic and diatomic species, indicating that the DIBs can be sensitive tracers of interstellar cloud conditions.

Key words: ISM: clouds – ISM: lines and bands – ISM: structure – stars: individual (rho Oph)

1. INTRODUCTION

Knowledge of the spatial distribution, dynamics, composition, and chemistry of neutral and ionized gas and dust is of fundamental importance in understanding the interstellar medium (ISM) and its relation to star formation. Through observations of absorption lines of atoms and small molecules at wavelengths ranging from radio to ultraviolet, the gaseous component of diffuse and translucent interstellar clouds has been probed in some detail and indicates that filamentary or sheet-like small-scale structure is common on scales as small as a few AU (Watson & Meyer 1996; Hartquist et al. 2003; Heiles 2007). In contrast, the distribution of large molecules and dust in the diffuse ISM is far less well characterized, although for denser regions insight has been gained through imaging of dust emission. Variations in diffuse interstellar band (DIB) strengths have previously been reported on distance scales down to a few parsecs (Points et al. 2004; van Loon et al. 2009), but over distance scales ∼10–150 AU, no significant variations have yet been observed (Smith et al. 2013; Rollinde et al. 2003). The results presented in the present study constitute the first detection of DIB variations over distances on the order of a few hundred AU.

Although the carriers of the DIBs remain to be identified (Herbig 1995; Sarre 2006), it is widely thought that the absorption features arise from electronic transitions in large gas-phase molecules which are associated with, and are possibly formed from, dust grains. The linking of diffuse band absorption to the presence of dust grains rests in significant part on the generally good correlation between their strengths and E_{B-V} although deviations are well established.

In order to probe the large-molecule/dust distribution in diffuse regions of Ophiuchus we have undertaken observations of DIBs toward four bright stars in the ρ Oph system (A, B, C, and DE)—as shown in Figure 1—the first results of which were described by Cordiner et al. (2005, 2006). Taking a distance to ρ Oph A and B of 111^{+12}_{-10} pc (van Leeuwen 2007), the stars comprising this binary are separated by a sky-projected distance of *c.* 344 AU. The stars ρ Oph C and DE are more distant at 125^{+14}_{-11} and 135^{+12}_{-10} pc (van Leeuwen 2007), and separated from ρ Oph AB by sky-projected distances ∼17,000 AU and ∼19,000 AU, respectively. An additional motivation for this work is investigation of the relative band strengths for closely aligned lines of sight as this could provide a new clue in the search for diffuse band assignments. Of particular importance in this regard, the physical and chemical conditions of very closely separated sightlines are expected to be similar to each other, thereby reducing the number of physical and chemical variables that may affect diffuse band strengths. In this Letter, we describe the detection of significant differences in DIB strengths of up to *c.* 9% between the closely spaced lines of sight toward ρ Oph A and B, and larger differences up to *c.* 40% between AB and ρ Oph C and DE, all four of which have the same E_{B-V} within ±0.01.

2. OBSERVATIONS

The ρ Oph system consists of five young early-to-mid B-type dwarf stars (Dommanget & Nys 1994), the basic properties of which are given in Table 1. Observations were carried out during the months of 2004 March and 2005 April using the University College London Echelle Spectrograph at the Anglo-Australian Telescope with a 1″ slit width. Complete wavelength coverage was obtained from 4600 to 10,000 Å, with a spectroscopic resolving power of 52,000–58,000. The median seeing was 0.″95 (2004) and 1.″7 (2005). This was sufficient for the ρ Oph AB pair to be resolved on both epochs, with at most 0.1% cross-contamination of flux in their reduced spectra (assuming Gaussian spatial profiles). The separation of ρ Oph DE is only 0.″6, but D dominates the spectrum because it is 1.2 mag brighter than E.

[3] Current address: Astrochemistry Laboratory and The Goddard Center for Astrobiology, Mailstop 691, NASA Goddard Space Flight Center, 8800 Greenbelt Road, Greenbelt, MD 20770, USA.
[4] Current address: Adler Planetarium, 1300 South Lake Shore Drive, Chicago, IL 60605, USA.

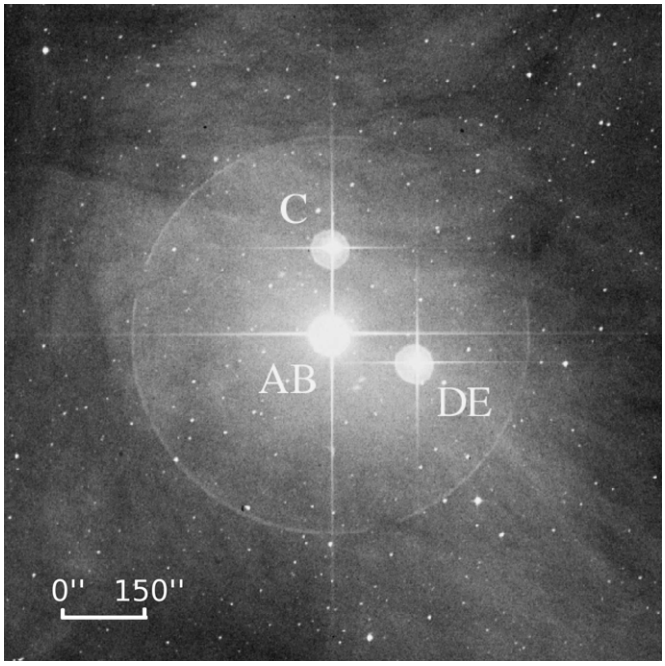

Figure 1. Photographic J (blue) image of the ρ Oph system obtained from the Digitized Sky Survey (DSS). Angular distances between components are as follows: $\theta(\mathrm{AB}) = 3\farcs1$, $\theta(\mathrm{AC}) = 150''$, $\theta(\mathrm{AD}) = 169''$, and $\theta(\mathrm{DE}) = 0\farcs6$.

Table 1
Program Star Properties

Star	HD	Spectral Type	V	E_{B-V}	S/N (6000 Å)
ρ Oph A	147933	B2/B3 V	5.0	0.47	1200
ρ Oph B	147934	B2 V	5.9	0.47	1100
ρ Oph C	147932	B5 V	7.3	0.47	800
ρ Oph D	147888	B3/B4 V	6.8	0.48	900

Notes. Spectral types are from the Michigan Catalogue of Spectral Types (Houk & Smith-Moore 1988). Reddening values (E_{B-V}) are from Pan et al. (2004).

The search for small-scale structure through DIB spectra is facilitated where there are similarities in stellar spectral type coupled with a low level of contaminating stellar photospheric features. The spectral match and stellar spectra are particularly good in the case of ρ Oph A and B, and the situation is generally satisfactory for comparison of AB with ρ Oph DE. The spectrum of ρ Oph C is contaminated by weak absorption features that are not present for the other stars. Short-timescale variability is detected in several of its Si II and He I lines, somewhat reminiscent of β Cephei-type or slowly pulsating B stars (see, e.g., Telting et al. 2006). Contamination of the observed ρ Oph C DIBs is negligible however, with the exception of λλ5780 and 5797.

Reduction and analysis techniques have been described previously in detail by Cordiner et al. (2006). Particular attention has been paid to nonlinearity in the CCD response, scattered light subtraction, telluric and blaze corrections. All four program stars were observed in immediate succession and without altering the optical setup of the telescope or spectrograph (during each night of observations), in order to maximize consistency between the recorded spectra. Exposure times were varied so as to obtain similar photon counts for each star; signal-to-noise ratios of the reduced spectra are given in Table 1.

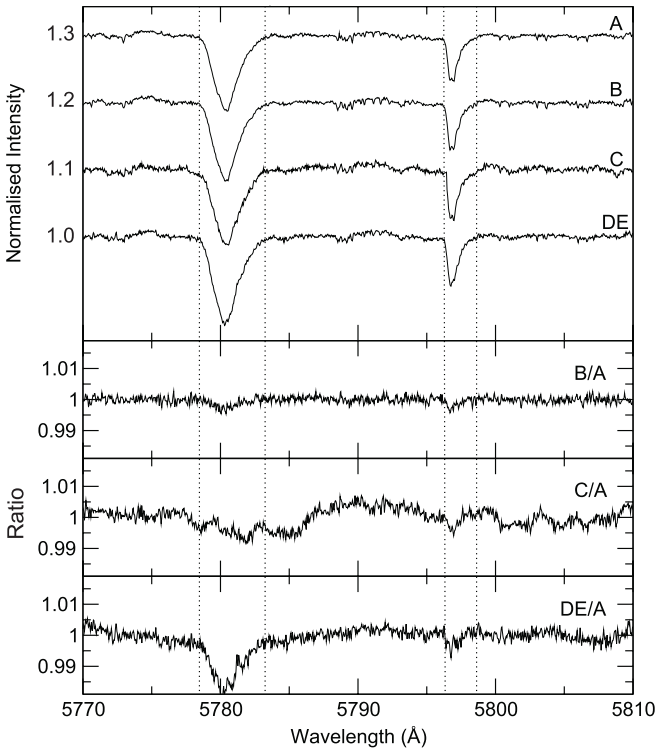

Figure 2. Spectra of the region covering the λλ5780 and 5797 diffuse bands. Top four panels are observations toward ρ Oph A, B, C, and DE, with ordinate offsets of 0.1; these are corrected for the blaze function but not for telluric effects and are unsmoothed. The three lower panels are non-blaze-corrected non-telluric-corrected ratios: $I_\lambda(\mathrm{B})/I_\lambda(\mathrm{A})$, $I_\lambda(\mathrm{C})/I_\lambda(\mathrm{A})$, and $I_\lambda(\mathrm{DE})/I_\lambda(\mathrm{A})$. The spectrum of ρ Oph C is significantly contaminated by weak stellar lines in this region. For a ratio X/A, a value <1 means the band is stronger along sightline X than A.

3. RESULTS AND DISCUSSION

3.1. Spectral Observations

Figure 2 shows the reduced (non-telluric-corrected) spectra (I_λ versus λ) in the wavelength region covering the λλ5780 and 5797 DIBs toward ρ Oph A, B, C, and DE. The lower three panels show the ratios $I_\lambda(\mathrm{B})/I_\lambda(\mathrm{A})$, $I_\lambda(\mathrm{C})/I_\lambda(\mathrm{A})$, and $I_\lambda(\mathrm{DE})/I_\lambda(\mathrm{A})$. The λλ5780 and 5797 DIBs are stronger, by 5% and 9%, respectively, toward B than A, as indicated by the residuals in the $I_\lambda(\mathrm{B})/I_\lambda(\mathrm{A})$ plot that precisely match the positions and profiles of the respective DIBs. These two bands are also stronger toward DE than A, but in this case λ5780 exhibits a much greater change in strength of ∼20%, the change for λ5797 being only *c.* 7%. This is a notable finding given that the values of E_{B-V} toward ρ Oph A and ρ Oph DE are almost identical with values of 0.47 and 0.48 (Pan et al. 2004). Despite contamination of the ρ Oph C spectrum, it is apparent that both λ5780 and λ5797 are stronger toward C than A.

Figure 3 (top panel) contains the corresponding data for λ6614 which again show this DIB to be slightly stronger toward ρ Oph B than A, and much stronger toward DE than A, in a similar fashion to λλ5797 and 5780. A significant *decrease* in λ6614 band strength is seen toward ρ Oph C relative to ρ Oph A. The λ6614 spectra appear to show some evidence of profile variation which may result from different carrier internal temperatures (Cami et al. 2004) or isotopic enrichments (Webster 1996).

Measurements of the equivalent widths for λλ5780, 5797, 6614, and seven other diffuse bands are given in Table 2. Broader DIBs are omitted due to the difficulty in accurately defining

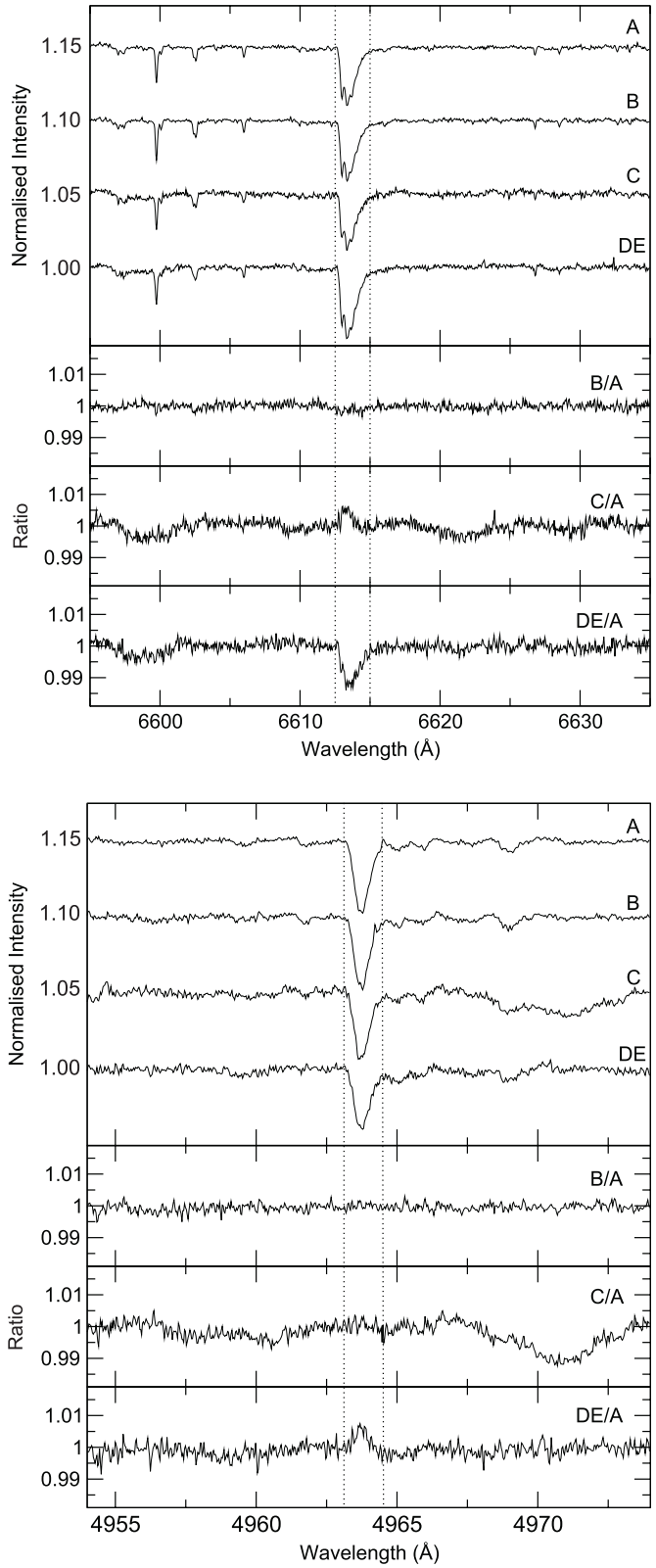

Figure 3. Spectra of the region covering the λ6614 diffuse band (top) and λ4964 "C_2" diffuse band (bottom). Data are as described in Figure 2 but with ordinate offsets of 0.05.

their continua in échelle spectra and the increased likelihood of overlapping stellar features. The results presented here for the yellow-to-red DIBs (obtained in 2005) match closely the results obtained by Cordiner et al. (2006), who used only the 2004 data (which had slightly lower signal to noise, but was observed with better seeing), and focused on DIBs at wavelengths >5500 Å. The fact that the spectra obtained on these two epochs match so closely despite the different instrumental setups and observing conditions adds confidence to the results presented here.

Table 2
ρ Oph Diffuse Interstellar Band and Atomic/Molecular Line Measurements

	A	B	C	DE	Error
Equivalent widths (mÅ)					
λ4726	99.3	97.8	112.9	67.4	4.3
λ4964	23.5	22.0	21.5	19.5	0.8
λ5780	188	197	[199]	227	2.8
λ5797	49.7	54.2	[56.0]	55.2	1.8
λ5850	29.8	31.9	35.2	25.2	1.8
λ6196	15.9	15.6	15.0	18.8	2.0
λ6203	42.0	42.5	43.0	47.2	6.0
λ6376	14.8	15.8	15.5	21.0	1.3
λ6379	27.1	28.3	28.5	34.7	1.3
λ6614	63.9	67.7	62.1	84.9	1.3
K I λ7699	88.1	89.5	77.7	90.5	0.3
Column densities and derived values					
N(H I)/10^{21}	4.3	...	...	4.9	1
$N(H_2)/10^{20}$	3.7	...	...	3.0	1
N(K I)/10^{12}	1.03	1.09	0.80	1.10	0.05
N(Ca I)/10^{10}	1.74	1.69	1.62	2.02	0.09
N(Ca II)/10^{12}	1.75	1.96	1.92	1.94	0.1
N(CH)/10^{13}	2.37	2.33	1.92	2.18	0.1
$N(CH^+)/10^{13}$	1.59	1.43	0.70	0.75	0.06
N(CN)/10^{13}	0.21	0.20	0.60	0.21	0.01
$N(C_2)/10^{13}$	4.1	2.9	3.3	4.0	1
$T_{rot}(C_2)$/K	51	49	46	56	1
n/cm^{-3}	625	450	1100	425	...
Depletion ($F*$)	1.09	...	...	0.88	0.07

Notes. Upper part of this table gives equivalent widths of interstellar features measured toward ρ Oph stars; values in brackets indicate probable stellar photospheric line contamination. The lower part of this table gives atomic and molecular column densities (in cm^{-2}) taken from Pan et al. (2004) except C_2 (from this work), H I, H_2, and depletion factor ($F*$) from Jenkins (2009). Gas number densities n are from the chemical model of Pan et al. (2005) and pertain to the CN-containing 2 km s^{-1} component only. The final column gives an average (±) error estimate on the respective values.

The λλ5780, 5797, 5850, 6379, and 6614 DIBs have the greatest central depths of those in our sample, and are the only ones to show a significant difference in strength between ρ Oph A and B. Small differences were measured for other bands toward these stars, but they are not significant given the noise level. Our data are consistent with all DIBs being slightly stronger toward ρ Oph B than A (by *c.* 5%). However, for the AB pair versus C and DE, the situation is more complex. Out of all the ρ Oph sightlines, we find that λ5850 is strongest toward C, whereas λ6614 is weakest. Additionally, DE has clearly the strongest λ6196 DIB, but the weakest λ4726 (the latter DIB is 40% weaker toward DE than C and 32% weaker than AB). This wide variation in behavior of different DIBs between the closely spaced sightlines in our sample shows that the carriers are being influenced by quite subtle variations in physical/chemical interstellar conditions.

An important advance in DIB studies was the identification of a set of DIBs that have a propensity to follow in strength the column density of diatomic carbon molecules—the so-called C_2 DIBs (Thorburn et al. 2003). A spectroscopic property of the C_2 DIBs (possibly related to the structure of their carriers) is that they fall predominantly at the blue end of the spectrum

($\lesssim$5500 Å), whereas the non-C_2 DIBs that we have measured fall at the red end (>5500 Å). Among the strongest of the C_2 DIBs is λ4964, data for which are shown in Figure 3 (bottom panel). This DIB shows no detectable difference between ρ Oph A and B but is found to be weaker toward ρ Oph DE than AB. Interestingly, we find that a total of nine out of the ten observed C_2 DIBs (λλ4726, 4734, 4964, 4984, 5176, 5418, 5512, 5541, and 5546) are measured to be weaker toward DE than AB (Smith 2006). The remaining λ5170 C_2 DIB is overlapped by a broad spectral feature, probably stellar in origin, which precludes a proper measurement of its variation. Ten out of eleven of the non-C_2 DIBs we observed in the yellow-to-red part of the spectrum (for which measured variations are larger than the errors), show the opposite trend, and are stronger toward DE than AB (data for λλ5705, 6660, and 7224 are given by Smith 2006), the single exception being λ5850. These results strongly support the association of the C_2 DIBs as a special group.

3.2. The ISM toward the ρ Oph Star System

Snow et al. (2008) studied the atomic (K I, Na I, and Ca I) column densities toward ρ Oph A, C, and D and determined the three-dimensional locations of these stars with respect to the ρ Oph cloud complex. They conclude that while ρ Oph AB and D are probably in front of the dense molecular cloud and probe a more diffuse portion, ρ Oph C more likely lies embedded in a CN-rich molecular part. As discussed by Snow et al. (2008), the ratio of total-to-selective extinction (R_V) is unusually high toward ρ Oph, and the far-UV rise is quite flat. These observations are consistent with the presence of relatively large dust grains and an absence of the very smallest grains (Seab & Snow 1995). Notably, the reported E_{B-V} values for the ρ Oph stars are almost identical (Table 1), which, given the magnitude of the observed DIB variations, is consistent with previous findings that the DIBs do not arise directly from the large grains that cause optical extinction (Sarre 2006).

3.3. Comparison of DIBs with Known Atoms and Molecules

A body of data for atoms and small molecules toward the ρ Oph stars is given in Table 2, where the column densities quoted are in general the sum over a number of blended velocity components. Unfortunately, the widths of the DIBs preclude their association with any particular component. We measured equivalent widths for 23 lines of C_2 in each of our spectra (in the range 7700–8900 Å, which covers the (2–0) and (3–0) C_2 vibrational bands). Total C_2 column densities were calculated using the oscillator strengths of Bakker et al. (1997); the best-fitting rotational temperatures ($T_{\rm rot}(C_2)$) were obtained using B. McCall's C_2 calculator (at http://dib.uiuc.edu/c2/), and are given in Table 2. All four lines of sight show absorption due to CN at around 2 km s^{-1}, with a common Doppler $b \approx 0.8$ km s^{-1}.

Apart from CH^+ which has a larger total column density toward ρ Oph A than B, the errors on the total column densities are too large to permit any clear distinction to be drawn between the properties of the gas toward ρ Oph A and B. However, if one considers only the main 2 km s^{-1} component, CH, CH^+, K I, and Ca II are all 10%–20% stronger toward B than A. Our high signal-to-noise K I equivalent width measurements also show more neutral potassium toward B than A. We infer that the column of DIB carriers increases toward ρ Oph B in concert with the species noted above. It is difficult, however, to know whether this is due to variations in the gas density, lower atomic (and DIB) depletions, changes in ionization equilibrium, or due to the geometric structure of the cloud.

Our observations toward ρ Oph C, as well as those of Pan et al. (2004) and Snow et al. (2008) show a relative underabundance of K I and Ca I compared with the other three sightlines. Consistent with its (∼3 times) greater CN column density, Snow et al. (2008) concluded that ρ Oph C is more deeply embedded in the dense, CN-rich material of the background (star-forming) molecular cloud. This relatively high density material should result in more depletion, which is the most likely explanation for the low K I and Ca I column densities. The lower λ6614 strength toward ρ Oph C may also be related to this depletion. The fact that the variations in the "red" DIB strengths are only on the order of a few percent for C compared with AB and DE shows that their carriers are, in general, not closely associated with CN. This result is in accordance with the study of λλ5797 and 5780 by Weselak et al. (2008). By contrast, the "blue" λ4726 DIB is very strong toward C, which confirms the association of its carrier with molecular material traced by C_2 (Thorburn et al. 2003).

The greater strengths measured for λλ5797 and 5850 toward ρ Oph C are consistent with the assignment of these DIBs to Krełowski & Walker (1987)'s group III, which is a family of diffuse bands that tend to have relatively narrow profiles. These "KWIII" DIBs (in contrast to those in the KWII group) are generally observed to be strongest in better shielded, denser diffuse clouds where the UV radiation field is weaker and small molecules are more abundant (Cami et al. 1997).

The sightline toward ρ Oph DE is relatively more diffuse than C, as indicated by the lower CN column density. It has a lower depletion factor ($F*$; Jenkins 2009) than A, indicative of a lower gas density. The 2 km s^{-1} component toward DE also has the lowest modeled density (Pan et al. 2005), consistent with it being the more diffuse sightline. The greater C_2 rotational temperature measured toward DE may reflect the increased (photo-electric) heating expected to result from a stronger UV radiation field pervading this more diffuse gas. As shown in Figure 2, the amount by which the λ5780 DIB strength increases between A and DE (∼20%), is greater than the amount by which λ5797 increases (∼10%). This pattern is consistent with the hypothesis (Krełowski & Walker 1987; Cami et al. 1997) that the carrier of the λ5780 DIB favors more diffuse environments than λ5797. The strengths of other DIBs in the same (KWII) group as λ5780 (λλ6196, 6203 and 6614) show a similarly large enhancement (∼20%) toward DE compared to A/B. With the striking exception of CH^+ (−26%), CH, Ca I, K I, and Ca II show increases in column density in the range 15%–30% (for the main 2 km s^{-1} component) from A to DE, which is analogous to their increase from A to B discussed earlier, and could plausibly be related to a lower degree of depletion in the gas toward DE.

The relative weakness of the C_2 DIBs toward DE is consistent with this being the more diffuse (and therefore, more molecule-poor) sightline of our sample. Our C_2 spectra are, however, of insufficient signal-to-noise to discern differences in the C_2 column densities between the ρ Oph sightlines; dedicated future C_2 observations will be required to confirm this.

4. CONCLUSIONS

Using high signal-to-noise échelle spectra of the stars ρ Oph A, B, C, and DE, the strengths of some of the observed DIBs are found to differ by about 5% on sky-projected distance scales less than *c.* 344 AU. The observed DIB strength variations between ρ Oph A and B are attributed to an increase in the abundances of their carriers/chemical precursors from A to B. Toward ρ Oph C and DE, the DIB behavior is more complex, probably as a result

of the greater differences in physical and chemical conditions in the ISM over the relatively larger distances between these sightlines and the different locations of these stars with respect to the background molecular cloud. The yellow/red DIBs are generally found to be strongest in the relatively diffuse, less-depleted gas toward ρ Oph DE. This is in striking contrast to the C_2 (blue) DIBs, which are consistently weaker toward DE than the other stars. The λ5850 DIB is found to be strongest in the more dense, depleted and molecule-rich diffuse gas toward ρ Oph C, consistent with its assignment to Krełowski & Walker (1987)'s group III.

Observed DIB strength variations are, in some cases, significantly greater in magnitude than the corresponding variations among atomic and (most) diatomic species; for example the equivalent widths of $\lambda\lambda$4726, 5780, and 6614 toward DE compared with A/B exceed the magnitude of variation in all observed species apart from CH^+. Such variations imply that diffuse band carrier abundances are very sensitive to variations in cloud conditions. Given the small distances between our observed sightlines, differences between the elemental compositions of their gases are expected to be negligible. Variations in diffuse band strengths and atomic and molecular column densities could therefore arise as a consequence of density inhomogeneity or the strength of the incident radiation field. Recent observations of CH^+ and SH^+ in the diffuse ISM have highlighted the importance of turbulent dissipation arising from shocks or velocity shears (Godard et al. 2009, 2012); this may also play a role in determining diffuse band carrier abundances on small distance scales, particularly if the carrier formation is driven by warm chemistry or through release of material from interstellar dust grains.

A more complete explanation for the origin of the observed small-scale variations in DIB strengths in the ρ Oph system will require a detailed knowledge of the properties of each sightline, including the density, temperature, (gas and solid-phase) chemical abundances and radiation field. This could be achieved through high signal-to-noise, high-resolution optical/UV/IR studies of atomic and molecular absorption lines including H I, H_2, C, C_2, and other neutral and ionic species sensitive to physical conditions in the ISM.

We thank PATT for the allocation of AAT time and T & S, EPSRC for studentships, and STFC for a visitor grant. M.A.C. thanks the NASA Astrobiology Institute through The Goddard Center for Astrobiology. S.J.F. thanks M. M. Dworetsky and I. D. Howarth for discussions on photospheric line-profile variations in ρ Oph C.

REFERENCES

Bakker, E. J., van Dishoeck, E. F., Waters, L. B. F. M., & Schoenmaker, T. 1997, A&A, 323, 469
Cami, J., Salama, F., Jiménez-Vicente, J., Galazutdinov, G. A., & Krełowski, J. 2004, ApJL, 611, L113
Cami, J., Sonnentrucker, P., Ehrenfreund, P., & Foing, B. H. 1997, A&A, 326, 822
Cordiner, M. A., Fossey, S. J., Smith, A. M., & Sarre, P. J. 2006, FaDi, 133, 403
Cordiner, M. A., Sarre, P. J., & Fossey, S. J. 2005, AAO Newsletter, 107, 9
Dommanget, J., & Nys, O. 1994, CoORB, 115, 1
Godard, B., Falgarone, E., Gerin, M., et al. 2012, A&A, 540, A87
Godard, B., Falgarone, E., & Pineau Des Forêts, G. 2009, A&A, 495, 847
Jenkins, E. B. 2009, ApJ, 700, 1299
Hartquist, T. W., Falle, S. A. E. G., & Williams, D. A. 2003, Ap&SS, 288, 369
Heiles, C. 2007, in ASP Conf. Ser. 365, SINS-Small Ionized and Neutral Structures in the Diffuse Interstellar Medium, ed. M. Haverkorn & W. M. Goss (San Francisco, CA: ASP), 3
Herbig, G. H. 1995, ARA&A, 33, 19
Houk, N., & Smith-Moore, M. 1988, Michigan Catalogue of Two-dimensional Spectral Types for the HD Stars, Vol. 4 (Ann Arbor, MI: Dept. of Astronomy, Univ. Michigan)
Krełowski, J., & Walker, G. A. H. 1987, ApJ, 312, 860
Pan, K., Federman, S. R., Cunha, K., Smith, V. V., & Welty, D. E. 2004, ApJS, 151, 313
Pan, K., Federman, S. R., Sheffer, Y., & Andersson, B. G. 2005, ApJ, 633, 986
Points, S. D., Lauroesch, J. T., & Meyer, D. M. 2004, PASP, 116, 801
Rollinde, E., Boissé, P., Federman, S. R., & Pan, K. 2003, A&A, 401, 215
Sarre, P. J. 2006, JMoSp, 238, 1
Seab, C. G., & Snow, T. P. 1995, ApJ, 443, 698
Smith, A. M. 2006, PhD thesis, The Univ. Nottingham
Smith, K. T., Fossey, S. J., Cordiner, M. A., et al. 2013, MNRAS, 429, 939
Snow, T. P., Destree, J. D., & Welty, D. E. 2008, ApJ, 679, 512
Telting, J. H., Schrijvers, C., Ilyin, I. V., et al. 2006, A&A, 452, 945
Thorburn, J. A., Hobbs, L. M., McCall, B. J., et al. 2003, ApJ, 584, 339
van Leeuwen, F. 2007, Hipparcos, the New Reduction of the Raw Data (Berlin: Springer)
van Loon, J. T., Smith, K. T., McDonald, I., et al. 2009, MNRAS, 399, 195
Watson, J. K., & Meyer, D. M. 1996, ApJL, 473, L127
Webster, A. 1996, MNRAS, 282, 1372
Weselak, T., Galazutdinov, G. A., Musaev, F. A., & Krełowski, J. 2008, A&A, 484, 381